Available online at www.sciencedirect.com
ScienceDirect
Journal of Nuclear Materials 375 (2008) 157–167
journal of nuclear materials
www.elsevier.com/locate/jnucmat

Enhanced thermal conductivity oxide nuclear fuels by co-sintering with BeO: II. Fuel performance and neutronics

Kevin McCoy *, Claude Mays

AREVA NP Inc., P.O. Box 10935, Lynchburg, VA 24506-0935, United States

Received 22 March 2007; accepted 22 October 2007

Abstract

The fuel rod performance and neutronics of enhanced thermal conductivity oxide (ECO) nuclear fuel with BeO have been compared to those of standard UO_2 fuel. The standards of comparison were that the ECO fuel should have the same infinite neutron-multiplication factor k_{inf} at end of life and provide the same energy extraction per fuel assembly over its lifetime. The BeO displaces some uranium, so equivalence with standard UO_2 fuel was obtained by increasing the burnup and slightly increasing the enrichment. The COPERNIC fuel rod performance code was adapted to account for the effect of BeO on thermal properties. The materials considered were standard UO_2, UO_2 with 4.0 vol.% BeO, and UO_2 with 9.6 vol.% BeO. The smaller amount of BeO was assumed to provide increases in thermal conductivity of 0, 5, or 10%, whereas the larger amount was assumed to provide an increase of 50%. A significant improvement in performance was seen, as evidenced by reduced temperatures, internal rod pressures, and fission gas release, even with modest (5–10%) increases in thermal conductivity. The benefits increased monotonically with increasing thermal conductivity. Improvements in LOCA initialization performance were also seen. A neutronic calculation considered a transition from standard UO_2 fuel to ECO fuel. The calculation indicated that only a small increase in enrichment is required to maintain the k_{inf} at end of life. The smallness of the change was attributed to the neutron-multiplication reaction of Be with fast neutrons and the moderating effect of BeO. Adoption of ECO fuel was predicted to provide a net reduction in uranium cost. Requirements for industrial hygiene were found to be comparable to those for processing of UO_2.

PACS: 28.41.Bm; 89.30.Gg

1. Introduction

The companion paper [1] discusses the processing and properties of enhanced conductivity oxide (ECO) nuclear fuel. This fuel form was produced by a co-sintering process, in which fine UO_2 powder was granulated, and the granules were coated with BeO, pressed, and sintered to produce fuel pellets. The processing approach produced a continuous BeO phase, with a volume fraction of roughly 5–10%. A 9.6% volume fraction increased the thermal conductivity 50% in unirradiated fuel pellets. This increase is consistent with previous results [2] with lower BeO volume fractions. This paper complements the companion paper by using codes for fuel rod performance and neutronics to predict the benefits of ECO fuel during irradiation. It also provides an initial assessment of how inclusion of BeO will affect requirements for industrial hygiene.

The fuel rod performance modeling followed the methods used in designing a 'reload', that is, a batch of fuel that replaces about one third of the assemblies in a power reactor. Conservative inputs were used to predict volume-averaged fuel temperatures, fission gas release, and fuel rod internal pressure throughout the life of a fuel rod. Fuel performance during a LOCA initialization transient was calculated for several discrete burnups.

The neutronic calculation was likewise similar to that for a commercial refueling. A transition from standard

* Corresponding author.

0022-3115/$ - see front matter © 2007 Published by Elsevier B.V.
doi:10.1016/j.jnucmat.2007.10.014

UO_2 fuel to ECO fuel was considered, with the ^{235}U enrichment being adjusted so that the lifetime energy extraction per fuel assembly and the core average k_{inf} at end-of-cycle would be equal for the two fuels.

2. Fuel rod performance modeling

Fuel rod performance for ECO fuel was calculated with AREVA's proprietary COPERNIC code [3]. COPERNIC performs the thermal-mechanical analyses necessary to accurately simulate the behavior of a fuel rod during its irradiation. Inputs to COPERNIC include rod manufacturing characteristics and irradiation conditions. Irradiation conditions, in turn, include thermal-hydraulic conditions and power histories. Outputs from COPERNIC include fuel temperatures, cladding temperatures, stresses and strains, internal pressures, and thicknesses of the corrosion products on the cladding. The program has received regulatory approval for use with UO_2, mixed oxide (UO_2–PuO_2), and UO_2–Gd_2O_3 fuels. The regulatory approval also covers methodologies for using COPERNIC to calculate fuel rod internal gas pressure, LOCA initialization, centerline fuel melting, cladding strain, cladding creep collapse initialization, and cladding peak oxide thickness. COPERNIC was not designed for use with ECO fuel, but it was adapted using the techniques described below.

COPERNIC provides a comprehensive description of the thermal-mechanical performance of a fuel rod. Its models cover heat production and transfer, fission gas release, pellet strains, cladding strains, cladding corrosion and hydriding, internal gas pressure, and the irradiation dependence of material properties. The thermal model includes submodels for the fuel pellet radial power profiles, fuel thermal conduction, closure of the diametral gap, heat transfer across the pellet-cladding gap, cladding thermal conduction (including the effects of corrosion products), and heat transfer from the cladding to the coolant. The models have been extensively benchmarked against experiments [3].

The COPERNIC code architecture uses the following general approach. The fuel rod is divided along the axial coordinate into discrete regions known as 'slices'. The slices are subdivided into discrete radial regions known as 'rings'. It is assumed that the properties of the fuel and cladding do not depend on the azimuthal coordinate. This slice and ring composite forms a quasi two-dimensional numerical framework for the mathematical analysis. Axial heat transfer is neglected, so the slices can be individually analyzed for each time step. When all of the slices have been analyzed, they are coupled, and quantities such as internal pressure and axial friction forces are determined. This general mathematical calculation sequence, which is performed at each time step, produces fuel rod predictions that accurately simulate fuel rod behavior.

The two primary components of the COPERNIC calculation are the thermal and mechanical analyses. The thermal analysis solves the heat equation numerically, with the various parameters, such as heat capacity and thermal conductivity, being determined from local characteristics of the fuel, such as temperature and local burnup. The mechanical model addresses the total strain as a function of position. The total strain includes a variety of contributions, including elasticity, creep, and densification. The strains are subject to compatibility constraints. Stresses are subject to the boundary conditions imposed by external pressures and to the constraints of axial symmetry [3].

Comparative calculations of fuel rod performance were performed with COPERNIC for UO_2 and ECO fuel. The calculations were based on a previous calculation for irradiation of Mark-B11 fuel in a Babcock & Wilcox reactor. Mark-B11 refers to a 15×15 fuel assembly design in which the fuel rod diameter is nominally 10.5664 mm (0.416 in.) rather than the 10.922 mm (0.430 in.) that is more commonly used in Babcock & Wilcox reactors. The calculations were intended to be typical of the irradiation of Mark-B11 fuel rather than to represent a given batch of fuel assemblies in a given reactor.

The COPERNIC code was used to track the conditions and performance of a fuel rod through three cycles of irradiation. The fuel rod geometry and operating conditions were generally nominal, with two exceptions that were designed to provide conservatism. These exceptions were the linear heat generation rate and the imposition of transients.

The performance of a fuel rod will depend on its linear heat generation rate as a function of burnup. Licensing and set point analyses typically use a composite linear heat generation rate rather than the actual linear heat generation rate of a single fuel rod. The composite is constructed in three steps. First, the maximum fuel rod average burnup for any rod in the batch is determined as a function of time. Second, the maximum linear heat generation rate for any rod in the batch is determined as a function of maximum fuel rod average burnup. Third, a curve is chosen that bounds the maximum linear heat generation rate as a function of the maximum fuel rod average burnup. For simplicity of analysis, the bounding curve may be taken to be a sequence of irradiations at constant linear heat generation rates, with relatively short transitions from one linear heat generation rate to the next. Fig. 1 shows the bounding curve that was used in the calculations reported here.

An operating power reactor will be subject to transients that will affect the fuel temperature and fission gas release. No attempt is made to predict the timing and severity of the actual transients that will be experienced during operation. Instead, licensing analyses conservatively represent these by imposing a fixed number of severe, hypothetical transients. The calculation reported here imposed three limiting 'Condition I' transients and one non-limiting 'Condition II' transient. The condition levels are as defined in ANSI/ANS-57.5 [4]. Condition I refers to 'events... that are expected frequently or regularly in the normal course of power operation. The design requirement for these events is that they shall be accommodated with margin between

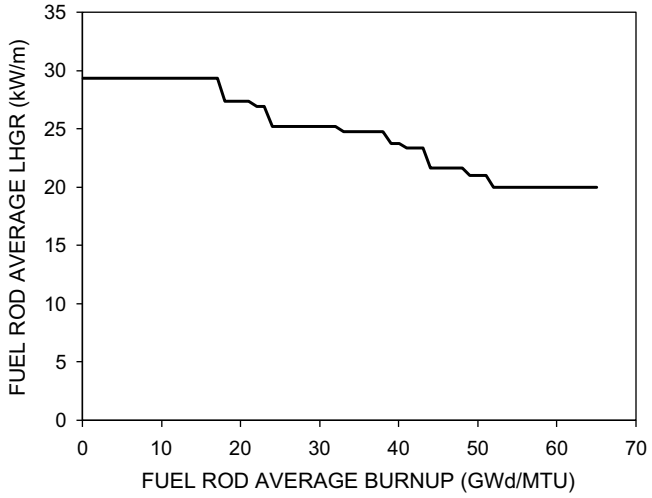

Fig. 1. Fuel rod average linear heat generation rate as a function of fuel rod average burnup for UO_2 fuel.

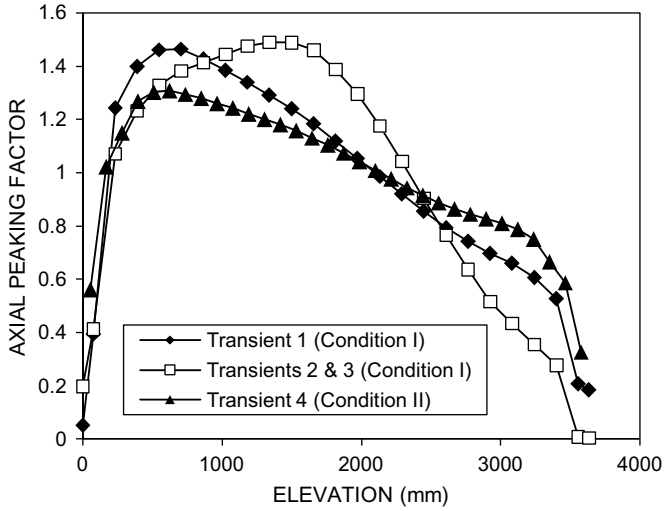

Fig. 2. Axial power shapes for transients used in performance calculations.

any plant parameter and the value of that parameter which would require either automatic or manual protective action'. Condition II refers to 'events... that are expected to occur during the life of a plant that may result in reactor shutdown. The design requirement for these events is that they shall be accommodated with, at most, a shutdown of the reactor with the plant capable of returning to power operation after corrective action'. Condition I and II transients are also known as 'operational transients' and 'events of moderate frequency', respectively. Neither Condition I nor Condition II events result in core damage.

Both types of transients, however, cause axial power peaking. The axial power shapes applied to the Condition I transients were limiting for Condition I, that is, they were characterized by the most severe axial power peaking that is consistent with operational limits. In contrast, the axial power shape applied to the Condition II transient was sufficient to cause reactor shutdown but had a less severe axial peak than the Condition I transients. The reduced peaking is due to the actions of the reactor control and protection systems, which limit the transient. Axial power shapes for the transients are shown in Fig. 2. The power shapes are presented in terms of the axial peaking factor, which is the linear heat generation rate at a given elevation divided by the average linear heat generation rate for the entire rod. Elevations are measured from the bottom of the active length of the rod. The transients provide substantial additional conservatism for the temperature, pressure, and fission gas release calculations in that they result in high local temperatures and large amounts of fission gas release.

Three axial power shapes were used for normal operation, as shown in Fig. 3. Shapes 1, 2, and 3, respectively, were used for the beginning, middle, and end of each operating cycle. Shape 1 is centrally peaked, as expected for a core that contains one batch of fresh fuel assemblies. The axial power shape then gradually progresses to shape 2 (flat) and then to shape 3 (end-peaked) as the core is

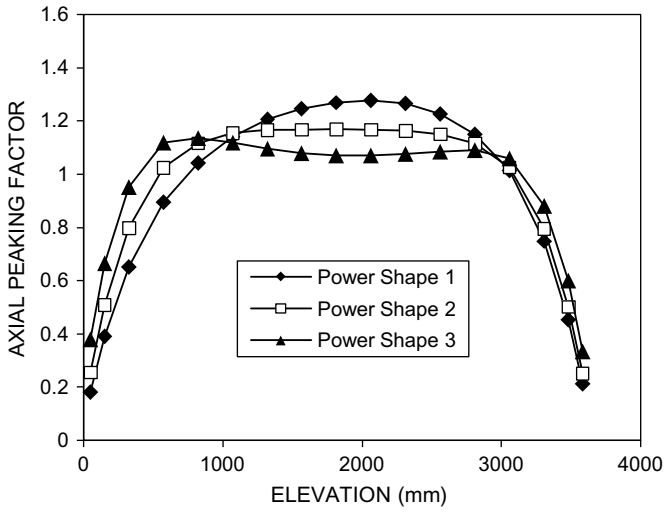

Fig. 3. Axial power shapes for normal operation.

depleted, particularly near the middle of the fuel rods, and the ends take over the load. The same sequence of axial power shapes was used for each cycle of irradiation.

The materials simulated with COPERNIC are described in Table 1. The standard UO_2 fuel represents current fuel material. ECO fuels with 4 vol.% BeO were assumed to provide increases in thermal conductivity of 0, 5, or 10%; these are denoted as ECO-4/0, ECO-4/5, and ECO-4/10,

Table 1
Compositions of fuel materials considered

Component	Fuel type		
	Standard UO_2 (%)	ECO-4/x (%)	ECO-10/50 (%)
UO_2	95.9	91.9	86.3
BeO	0.0	4.0	9.6
Closed porosity	4.0	4.0	4.0
Open porosity	0.1	0.1	0.1

respectively. These are collectively called ECO-4/x. ECO fuel with 9.6 vol.% BeO (ECO-10/50) was assumed to provide an increase in thermal conductivity of 50%. ECO-10/50 corresponds to the ECO-10 fuel discussed in the companion paper. The ECO-4/x fuels represent a less aggressive approach to incorporating BeO into the fuel and a more conservative estimate of its benefits.

It was decided at the outset that the calculations for ECO fuel should use it as a direct replacement for standard UO_2 fuel. In other words, the intended use of ECO fuel was that it should directly replace standard fuel on an assembly-for-assembly basis. Therefore, ECO fuel should provide (1) the same lifetime energy extraction per fuel assembly and (2) the same core thermal power as standard fuel. If ECO fuel were used in this way, the amount of steam provided to the turbine and the number of spent fuel assemblies produced per operating cycle would be identical for standard and ECO fuels. Any improvement in fuel rod performance, such as decreased fuel temperatures or end of life internal pressure, could then be used in support of reactor performance improvements, such as increased burnup or a power uprate.

COPERNIC was designed and licensed for commercial fuel. It was, therefore, a significant challenge to use COPERNIC in a way that represents an experimental fuel material such as ECO fuel. Fig. 4 is a schematic comparison of the two materials that explains how the challenge was met. The approach reflects the specific design and capabilities of COPERNIC. The upper portion of Fig. 4 compares the volume fractions of different materials in the fuel pellets. In ECO fuel, some of the UO_2 is replaced by a non-fissile material, such as BeO, which does not contribute significantly to power production. However, if ECO fuel is to be a direct replacement for standard fuel, the power produced by the UO_2 must be the same for both fuels, as shown in the lower portion of Fig. 4. Since the ECO fuel contains less total UO_2, it must have a greater end of life burnup to maintain the lifetime energy extraction per fuel assembly.

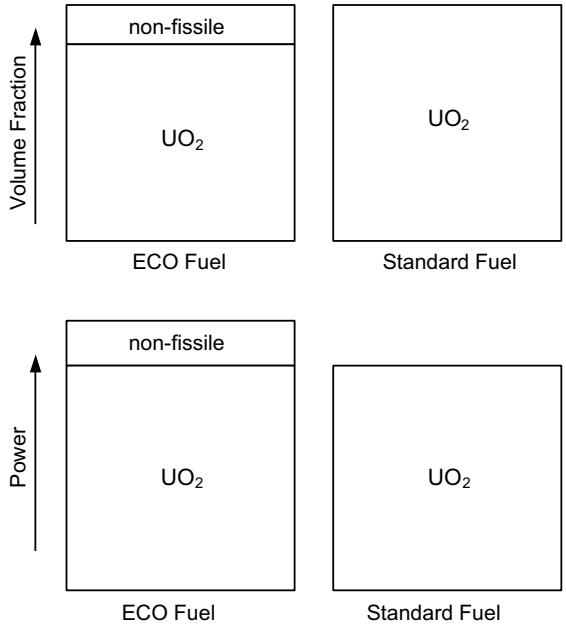

Fig. 4. Schematic comparison of volume fraction and linear power for ECO and standard fuels for calculations with COPERNIC.

Various approaches could be used in an attempt to simulate ECO fuel in COPERNIC. Most of the relevant inputs that can be changed in COPERNIC are related to the fuel rod and fuel pellet geometry or to the volume fraction of open and closed porosity. Adjusting these inputs would tend to have undesirable side effects because they affect the amount and location of void volume or the thermal conductivity of fuel. Such changes would, in turn, affect fuel rod performance, and the changes in fuel rod performance would not be clearly related to the replacement of UO_2 by a non-fissile material. The selected approach, which is suggested in Fig. 4, was to treat the non-fissile material as if it were additional UO_2 that produced additional (fictitious) power. The additional power would mean a greater burnup at end of life, which was as desired. However, the power would also affect the fuel temperature and fission gas release unless it were disposed of properly.

The question of how to handle the extra, fictitious power is best answered by using the ECO-4/x fuels as an example. As is shown in Fig. 4, the actual UO_2 is assumed to generate the same power in both the ECO-4/x and standard fuels. However, Table 1 notes that standard fuel is 95.9 vol.% UO_2 whereas the ECO-4/x fuel is 91.9 vol.% UO_2. The total power of an ECO-4/x fuel rod is therefore $95.9/91.9 = 1.0435$ times that of a standard fuel rod, that is, there is an additional 4.35% of fictitious power that is attributable to the non-fissile material. There is also 4.35% of additional, fictitious, fission gas production. COPERNIC allows direct correction for both of these effects. Fission gas release was adjusted by using a multiplier for the fission gas release model. The multiplier was set to $1/1.0435 = 0.9583$. Linear power was adjusted by using a COPERNIC input variable that specifies the fraction of fission energy deposited inside the fuel rod. For standard fuel, this fraction was 97.3%, with the remaining 2.7% being transferred directly to the coolant by gamma radiation or neutron kinetic energy. For ECO-4/x fuel, the fraction of fission energy deposited inside the fuel rod was set to $97.3\%/1.0435 = 93.24\%$. This adjustment hinges on the distinction between linear heat generation rate, which is the thermal power (per unit length of fuel rod) that is conducted through the surface of a fuel rod, and linear power, which is the thermal power generated per unit length of fuel rod. Similar adjustments were applied for the ECO-10/50 fuel. In that case, the multiplier on rod power (power factor) is $9.59/86.3 = 1.1112$.

Part of the COPERNIC input is a list of irradiation times and the burnups achieved at those times. To account for the increased linear power, the burnups for the ECO fuels were scaled by the appropriate power factors, but the times were left unchanged. Thus, for the ECO fuels,

the curve for LHGR as a function of burnup is similar to that shown in Fig. 1, but the curve is stretched to higher burnups.

An additional minor correction is required. The additional, fictitious thermal power from ECO fuel results in increased changes in coolant temperature as it flows past the fuel rod. The coolant flow rate was multiplied by the appropriate power factor to maintain the coolant temperature. The increase in coolant flow is fictitious, like the increase in linear power, so no actual changes in reactor coolant flow would be required to accommodate ECO fuel.

3. Effect on fuel temperatures

COPERNIC was used to simulate both standard UO_2 fuel and ECO fuel. It was assumed that ECO fuel provided enhancements in thermal conductivity that varied from 0 to 50%. The adjustments in thermal conductivity serve to indicate the magnitudes of the trends that will result from a change in thermal conductivity. The calculation with no increase in thermal conductivity was used to test the validity of the approach to handling the addition of non-fissile material that is described above.

Fuel temperatures as a function of burnup are given in Fig. 5. The temperatures are volume averages for the pellets in an entire fuel rod. It will be observed in Fig. 5 that the ECO-4/x and ECO-10/50 fuel rods attain end of life burnups of about 67.8 and 72.2 GWd/MTU, compared to about 65 GWd/MTU for standard UO_2 fuel. This reflects the reduced amount of UO_2 in ECO fuel and the requirement for the same energy lifetime extraction per fuel assembly.

The fuel temperatures exhibit a small increase at the beginning of life, followed by a gradual decrease for burnups up to about 12 GWd/MTU. Inspection of the results from COPERNIC reveals that these changes in temperature reflect changes in the size of the fuel-cladding gap.

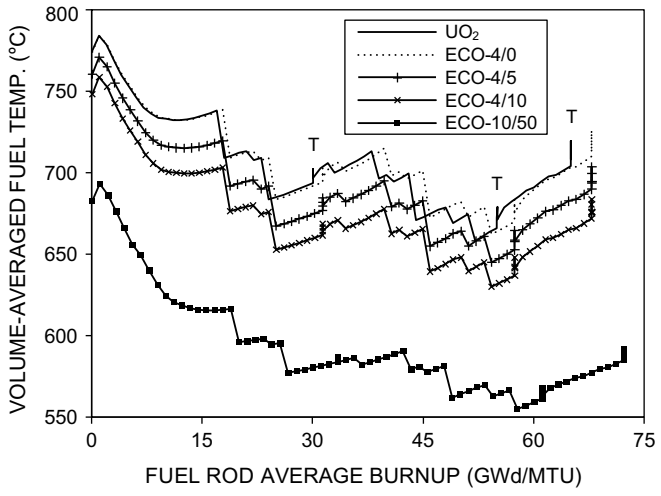

Fig. 5. Volume-averaged fuel temperatures as a function of fuel rod average burnup for standard UO_2 fuel and ECO fuels.

The gap initially widens, and its thermal resistance increases, as the fuel pellets densify. The gap subsequently narrows as the cladding creeps down onto the fuel pellets and the fuel pellets swell. As a result, the thermal resistance of the gap decreases, and the fuel temperature drops. The remainder of each temperature plot has a characteristic saw-toothed shape. There is a general alternation between gradual increases in temperature and relatively abrupt drops. This shape reflects the plateaus and slopes of the linear heat generation rate, which are shown in Fig. 1. The gradual increases in temperature correspond to the plateaus in the linear heat generation rate. The increases reflect the gradual degradation of the thermal conductivity of UO_2 with increasing burnup. The relatively abrupt decreases correspond to the slopes in the plot of the linear heat generation rate. Decreases in linear heat generation rate result in decreases in fuel temperature. The Condition I and II transients result in temperature spikes. For the base case, the spikes are labeled with the letter 'T' in Fig. 5. Only three spikes are visible in the figure because the last Condition I and the Condition II transients, both at end of life, cannot be resolved at the scale of the figure.

The standard UO_2 and ECO-4/0 fuels provide a useful check to determine whether it is realistic to simulate ECO fuel by producing extra power and transferring it directly to the coolant. Over certain ranges of burnup, notably from 0 to 17 GWd/MTU and 60–65 GWd/MTU, these fuels are operated at the same linear heat generation rate. It is observed from Fig. 5 that, within these ranges, the two fuels have very similar temperatures for a given burnup. This is exactly as expected. However, the COPERNIC model includes the gradual degradation of fuel thermal conductivity with burnup, and the ECO-4/0 fuel has a slightly greater burnup at end of life, so it also has a slightly higher temperature at end of life. Therefore, it can be concluded that the scheme for simulating ECO fuel is realistic.

Fig. 5 shows that an increased thermal conductivity has a marked effect on fuel temperature. ECO-4/0 fuel shows an increase in volume-averaged fuel temperature of about 6 °C at end of life relative to standard fuel. In contrast, ECO-4/5 and ECO-4/10, and ECO-10/50 fuels have temperatures that are about 15 and 33 °C, respectively, lower than that of standard fuel at end of life, whereas the temperature for ECO-10/50 fuel is a remarkable and 122 °C lower. For the ECO-4/x fuels, the results suggest that an enhancement in thermal conductivity by as little as 2% will provide some reduction in fuel temperature at end of life.

The benefits of increased thermal conductivity on centerline fuel temperatures should not be underestimated. As an example, consider the transient for ECO-4/x fuels at a burnup of about 31.3 GWd/MTU. At the end of the transient, the ECO-4/5 fuel has a volume-averaged fuel temperature that is about 18 °C below that of the ECO-4/0 fuel. In contrast, the corresponding difference in peak centerline fuel temperature between these cases is greater than 60 °C.

4. Effect on fission gas release and internal rod pressure

Additional results from the COPERNIC calculations reported above included fission gas release and fuel rod internal pressure as functions of burnup. These results are plotted in Figs. 6 and 7.

It is notable that Figs. 6 and 7 both lack the characteristic saw-toothed shape of Fig. 5. For fuel rod internal pressure, this might be partially explained by the location of the void volume. The void volume is predominantly in the upper plenum, with some contribution at low burnups from the fuel-cladding gap. The gas temperature in both of these regions is largely decoupled from the volume-averaged fuel temperature. The fission gas release curves, however, show that there is more to the story. As an example, note from Fig. 1 that there is a change in linear heat generation rate between burnups of 43 and 44 GWd/MTU for UO_2 fuel. That drop is reflected in a significant drop in fuel temperature, as shown in Fig. 5. However, Fig. 6 shows essentially no change in fission gas release over the same range of burnups. The reason is that fission gas release is determined not only by the current temperature but also by microstructural properties, such as the concentration of fission gas on the grain boundaries, that reflect the past history of the fuel.

Figs. 6 and 7 show that, compared to standard fuel, all the ECO fuels have improved performance with regard to fission gas release and fuel rod internal pressure. Relative to standard fuel, which releases 19.6 % of its fission gas at end of life, the ECO-4/0, -4/5, and -4/10 fuels have end of life fission gas release that is decreased by 1.7%, 4.0%, and 6.0%, respectively. The ECO-10/50 fuel has an end of life fission gas release only 4.5%. Similarly, the ECO-4/x fuels have end of life internal pressures that are 0.5, 2.0, and 3.3 MPa below those of standard fuel, whereas the ECO-10/50 fuel has a reduction of 9.1 MPa. These improvements are significant because they relax the constraint of fuel rod internal pressure on fuel design and reactor operation.

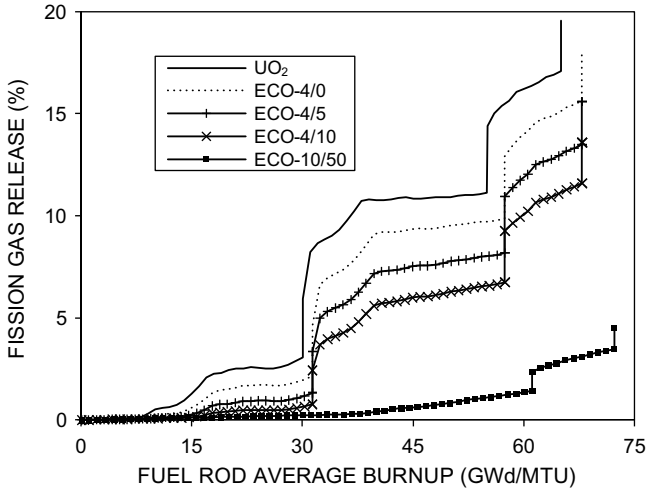

Fig. 6. Fission gas release as a function of fuel rod average burnup for standard UO_2 fuel and for ECO fuels.

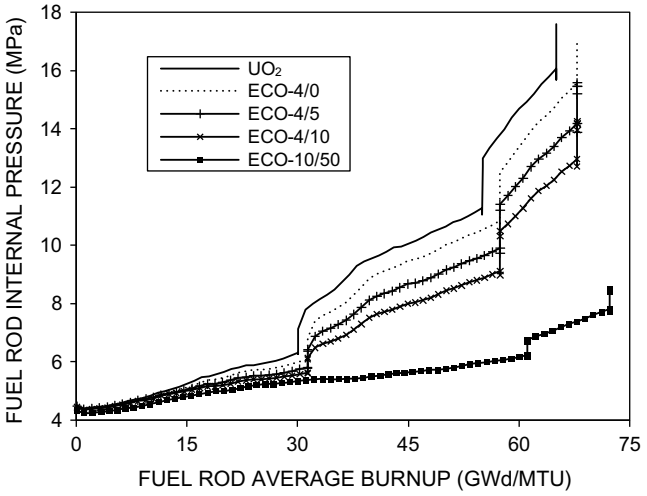

Fig. 7. Fuel rod internal pressure as a function of fuel rod average burnup for standard UO_2 fuel and for ECO fuels.

The plots for fission gas release and fuel rod internal pressure generally diverge with increasing burnup. The divergence is in agreement with the concept of fission gas release as an autocatalytic phenomenon, that is, that the release of some fission gas promotes release of more gas.

The results of the COPERNIC calculations show that even relatively small improvements in fuel thermal conductivity provide significant improvements in fuel rod performance. The improvements in thermal conductivity that are discussed here are comparable to those measured for unirradiated ECO fuel [1]. If the measured improvements are sustained under irradiation, they will provide the fuel designer and reactor operator with additional flexibility to increase power output or burnup, or to increase conservatism and safety.

5. Effect on LOCA initialization

Loss of coolant accident (LOCA) initialization calculations were performed to provide a comparison of standard UO_2 fuel and ECO fuel under conditions of LOCA initialization.

LOCA performance is regulated by 10 CFR 50.46, which provides acceptance criteria for emergency core cooling systems for light-water nuclear power reactors. Among the criteria are requirements that the calculated maximum fuel element cladding temperature shall not exceed 2200 °F (1204 °C) (10 CFR 50.46(b)(1)) and that changes in core geometry shall be such that the core remains coolable (10 CFR 50.46(b)(4)).

Designing to meet the LOCA criteria is complex and generally beyond the scope of this paper. However, some rules of thumb have been developed to help simplify the process. One such rule is that if the best-estimate volume-

average fuel temperature before the LOCA does not exceed 2050 °F (1121 °C), the cladding temperature will not exceed 2200 °F during the LOCA. The difference of 150 °F (83 °C) provides a margin for uncertainties in the best-estimate temperature and any temperature increase due to decay heat. A second rule of thumb is that, if the pressure inside the fuel rods before the LOCA does not exceed a certain level, the core geometry will remain coolable during the LOCA. Lower fuel rod internal pressures result in slower ballooning of the cladding and therefore less flow blockage, that is, less tendency for the fuel to assume a geometry that is not coolable. The rules of thumb do not replace a full LOCA analysis. Instead, they provide a relatively quick means for setting tentative fuel operational limits. Those limits are then confirmed by a full analysis.

Fuel rod performance for LOCA initialization was calculated using a best-estimate model for the limiting fuel rod. The linear heat generation rate as a function of burnup was similar to that used for analysis of fuel temperature or fission gas release, but the Condition I and Condition II operational transients were replaced by a single LOCA initialization transient. The strength of the transient is adjusted until the fuel reaches one of the limits for temperature and pressure given above. In the case of volume-average fuel temperature, the average is that for the hottest of COPERNIC's slices, which is typically at or just above the elevation of the axial power peak for the transient. The fuel rod performance calculation was stopped at the end of the LOCA initialization transient.

Fuel that can sustain a stronger transient without exceeding the limits is preferable because it performs acceptably under a wider range of operating conditions. The increased flexibility in operating conditions promotes plant profitability in that it helps to avoid shutdowns or restrictions on power output.

Many individual fuel rod performance calculations are needed for an analysis of LOCA initialization. First, LOCA performance depends on burnup, so the calculations must be performed at various times in life. Second, at each burnup, several transients with different axial power shapes are considered because the effect of the transient depends on its elevation in the core. Third, the strength of the transient must be adjusted so that the fuel reaches but does not exceed the rule-of-thumb limits.

The LOCA initialization transients were assumed to occur at 0.002, 18, 35, 45, and 62 GWd/MTU for standard UO_2 fuel or at equivalent energy extractions for ECO fuel. In each case, the burnup specified is that at the end of the transient. Each transient included a short ramp followed by sustained high power for a longer time. The duration of the ramp was 0.01 MWd/MTU, which corresponded to about 15–25 s, depending on the power level. For the transient at beginning of life (0.002 GWd/MTU), the period of sustained high power lasted for an exposure of 1 MWd/MTU, or a time of about 25 min. For the other times in life, the duration of the transient was 100 MWd/MTU, or a time in the range of 45–65 h. An unusually long duration was chosen to ensure that the effects of the transient had saturated.

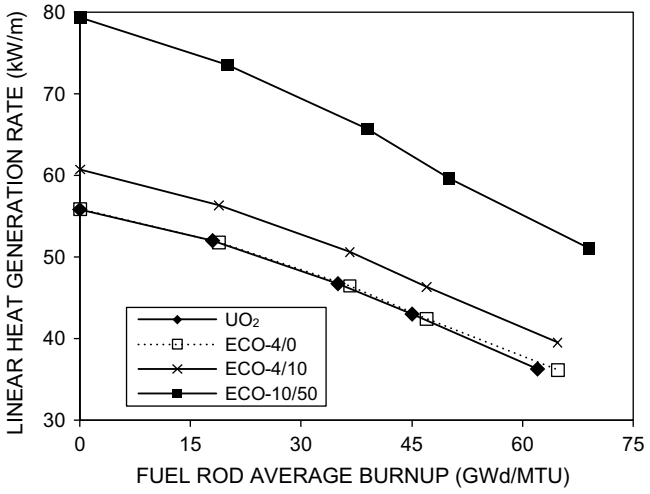

Fig. 8. Maximum local linear heat generation rate for LOCA initialization.

The LOCA initialization calculations used the same basis as the previous calculations on fuel temperature and fission gas release. In particular, the same fuel design, enrichments, and linear heat generation rate were used. The volume fractions of UO_2, porosity, and non-fissile, high-conductivity phase were likewise identical to those used previously, as were the corrections to FHEAT, coolant flow rate, and fuel enrichment for ECO fuel. The calculations included standard UO_2, ECO-4/0, ECO-4/10, and ECO-10/50 fuels.

The results of the calculation are shown in Fig. 8. The reported linear heat generation rate is the local rate at the axial peak of the transient rather than a fuel rod average. As in the previous calculations on fuel temperature and fission gas release, the burnups for the ECO fuel are slightly greater than those for the standard UO_2 fuel to promote comparisons at the same level of energy extraction. It is seen from Fig. 8 that the results for ECO-4/0 fuel are very similar to those for standard UO_2 fuel. This result is as expected. In contrast, ECO fuels with increased thermal conductivity provide a significant benefit for LOCA performance. When compared to standard UO_2 fuel, the ECO-4/10 fuel provides an increase in the maximum linear heat generation rate that varies from 4.9 kW/m at beginning of life to 3.2 kW/m at end of life. The corresponding increases for ECO-10/50 fuel are 23.5 and 14.8 kW/m, respectively.

6. Effects on neutronics

Adding a second phase with high thermal conductivity to a fuel pellet will change its neutronic properties, so those changes were analyzed to determine how they affect fuel performance. To the extent practical, the performance analysis of the ECO fuel was parallel to the design of a

commercial fuel reload. Some aspects of the process were simplified to reflect the exploratory nature of the work. This section describes the neutronic analysis process and provides the results of the analysis.

The approach was to simulate four operating cycles in which a power reactor undergoes a conversion from standard UO_2 fuel to ECO fuel. A baseline calculation was first performed in which UO_2 fuel was used for all cycles. That was followed by similar calculations for the conversion from UO_2 fuel to ECO fuel. The ECO fuel assemblies were assumed to be the same as the UO_2 fuel assemblies except for the pellet material and ^{235}U enrichment. It was also assumed that there was no mixing of standard UO_2 and ECO fuel rods in a single assembly. It is expected that substantial additional benefits would be realized by using the ECO fuel only for the fuel rods with the highest local power.

To make the neutronic calculations as realistic as possible, they were based on four refueling cycles of a 177-assembly Babcock & Wilcox reactor. The reactor was fueled with Mark-B9ZL assemblies. The Mark-B9ZL features 'zone loading', that is, the fuel rods have two different ^{235}U enrichments. The zoning is as shown in Fig. 9; there are reduced enrichment rods in the four locations adjacent to the instrument tube and in the twelve locations closest to the corners. Actual operating data for a commercial reactor were used. The reactor was chosen because it met two criteria. First, it had used the same fuel design for several cycles and therefore had an 'equilibrium core'. If a non-equilibrium core had been used instead, the comparisons could produce spurious results associated with cycles during the conversion. Second, the reactor does not use integral burnable absorbers, so its fuel enrichments are relatively low. ECO fuel may require increased enrichments to offset the reduction in uranium loading, but the enrichments must remain below the 5 wt% license limit that currently applies to commercial fuel facilities in the United States.

The reactor that was simulated uses 18-month refueling cycles and a very low leakage fuel shuffle scheme. This scheme is called 'in-in-out' because the fuel assemblies spend their first two cycles near the center of the core and are moved to the periphery for the third. Having the most heavily burned fuel on the periphery reduces neutron leakage from the core.

Fig. 10 shows a quarter-core map for the final cycle of the simulations. The map illustrates the in-in-out shuffle scheme. Note that there are too few peripheral locations for all the third-cycle assemblies, so some of them are placed in interior locations.

It is necessary to simulate four cycles because typical reactor reloads replace about one third of the fuel after each cycle. In addition, reinserted fuel was involved from an earlier cycle. For the conversion to ECO fuel, the four cycles represented, respectively, reactor operation with 60, 116, 176, and 177 of the core locations occupied by ECO fuel assemblies. Comparisons were made for the fourth cycle, when the reactor was fueled with a full core of either UO_2 fuel or ECO fuel. Utilities will normally not accept fuel that will reduce the length of their operating cycles, so the cycle length and the lifetime energy extraction per assembly were kept constant. Part of the fuel volume in ECO fuel is occupied by the non-fissile, high-conductivity second phase, so the ECO fuel has a lower uranium loading than standard UO_2 fuel. As a result, increases in burnup and ^{235}U enrichment are required to maintain cycle length. The loss of UO_2 loading in ECO fuel can be offset to some extent by the reduced fuel temperatures, which reduce Doppler absorption. There is also a neutronic benefit from the neutron multiplication reaction of ^{9}Be with fast neutrons.

CASMO-3 [5] was used for neutronic calculations for both standard fuel and UO_2–BeO fuel. This code represents the core with an averaged fuel assembly and gives the infinite neutron-multiplication factor k_{inf} as a function of burnup. Additional calculations were performed using

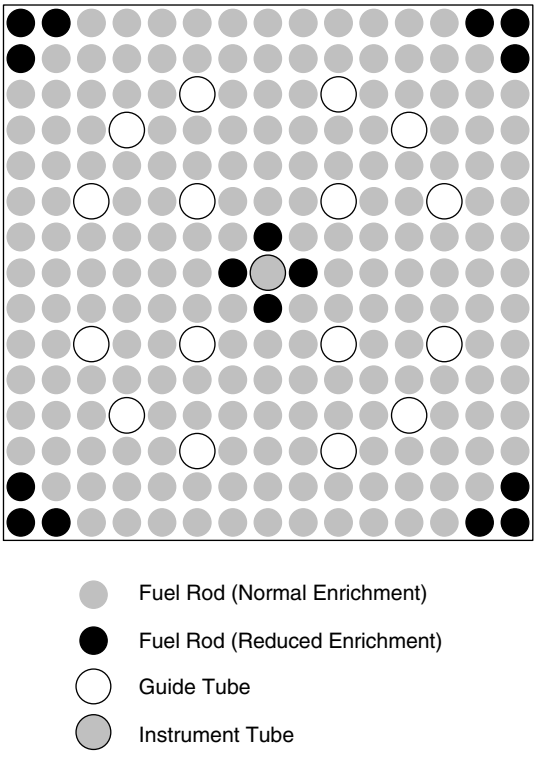

Fig. 9. Zoning of Mark-B9ZL fuel assembly.

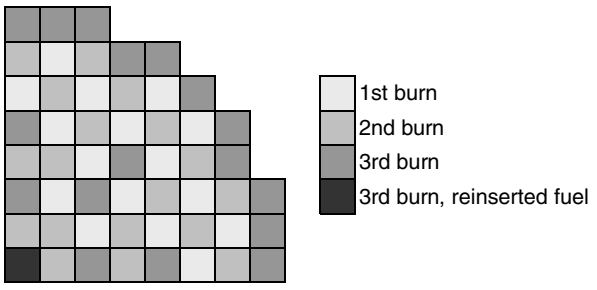

Fig. 10. Quarter-core map for final cycle.

Table 2
Fuel enrichments for standard UO_2 fuel case, final cycle

Batch	Irradiation cycle	# of assemblies	Average ^{235}U enrichment
A	Third burn, reinserted fuel	1	4.027
B	Third burn	56	4.027
C	Second burn	60	4.007
D	First burn	60	4.027

Table 3
Fuel densities for design comparisons

Phase	Fuel type	
	UO_2–BeO (%)	UO_2 (%)
UO_2	93.2	95
BeO	4.8	–
Voids	2	5

the TRITON control module of SCALE 5.0 [6] with the 238-energy group cross-section library. The TRITON code performs a more detailed calculation with fewer approximations than CASMO-3. For example, it uses a much finer energy-group structure for the cross section library, and will also perform depletion calculations (with the ORIGEN-S module of SCALE 5.0) for the beryllium, whereas CASMO-3 will not treat the beryllium as depletable. Both the finer energy-group structure and the use of ORIGEN-S mean that TRITON is more capable of treating the neutron multiplication reactions of beryllium. TRITON was also used for neutronic calculations for both standard fuel and UO_2–BeO fuel. Comparison of the results from TRITON and CASMO-3 allowed a correction for potential systematic errors that could arise from the use of CASMO-3's less detailed cross-section library.

The simulated end-of-cycle worth of a doped fuel rod with CASMO-3 and TRITON was used to establish a k_{inf} correction and ultimately an end-of-cycle enrichment correction for the CASMO-3 fuel assembly depletions. The enrichment correction was used for the fuel cycle economics calculation.

Information about the core for the fourth cycle is given in Table 2. The enrichments given are for standard UO_2 fuel. A comparison of fuel types is given in Table 3. The UO_2–BeO fuel has smaller volume fraction of voids than the standard fuel; this difference reflects differences in processing of the two fuel types. It has generally been observed that it is easier to sinter UO_2–BeO fuel to high density and to produce a continuous network of the second phase.

Substitution of UO_2–BeO fuel for UO_2 fuel required an increase in enrichment by only 0.0073 wt% to maintain the end-of-cycle value of k_{inf}. The smallness of the increase is presumably related to the neutron multiplication reaction of ^9Be and the moderating effect of BeO.

The consumption of ^9Be through neutron-multiplication reactions is small. It was found that only 0.15% of the initial ^9Be isotopic concentration was consumed over three cycles of irradiation.

Table 4
Effect of changes in fuel design on uranium cost

Fuel type	Number of assemblies	^{235}U Enrichment	Change in U cost, $	Total U loading, kg
UO_2 (base)	60	4.027	–	27820
UO_2–BeO	60	4.034	−501000	27290
UO_2 (base)	56	4.277	–	25970
UO_2–BeO	56	4.284	−506000	25470

7. Effects on economics

Economic comparisons were completed for four cases. Uranium costs were calculated with the SWUcalc 2.0 code [7] under the following assumptions: Enrichment was assumed to cost $110/SWU (separative work unit). Uranium feed was assumed to cost $53.5/kg U. The enrichment of the tails was assumed to be 0.3 wt% ^{235}U. The results of the economic comparisons reflect these assumptions and are given in Table 4. The changes in uranium cost and total uranium loading are for a full batch of fuel.

The first two cases provide a comparison of UO_2 and UO_2–BeO fuel for the final cycle of the simulation. These cases assumed a reload with 60 assemblies. As is reported in Table 4, the UO_2–BeO fuel requires an increase in ^{235}U enrichment of 0.0073 wt% to maintain lifetime energy extraction. However, the density of uranium is reduced in the ECO fuel, so the net result is a decrease in uranium cost of about $501 000 per batch.

The third and fourth cases are like the first two, but it is assumed that a reload of 56 assemblies would be acceptable. A reduction in the reload batch size from 60 to 56 is expected to impose penalties in terms of increased power peaking, but these may be acceptable with ECO fuel because of its improved thermal conductivity. It was also assumed that an increase in the ^{235}U enrichment by 0.25 wt% would be required to maintain lifetime energy extraction. The same increase in enrichment was assumed to apply for both fuel types. The increase in enrichment was strictly an engineering judgment and was not supported by a specific neutronic analysis or core design. With a 56-assembly batch, the decrease in uranium cost was $506 000 per batch for UO_2–BeO fuel. The cost advantage of UO_2–BeO fuel is therefore similar for the two batch sizes.

Table 4 does not directly compare the costs of the UO_2 base cases with 60 and 56 assemblies because those cases reflect a change in fuel cycle design rather than in materials. The total change in cost between the two UO_2 cases will reflect a reduction in manufacturing cost and an increase in uranium cost because of the increased enrichment. The net savings from reducing the batch size is estimated to be between $100 000 and $200 000.

The discussion above shows that substitution of ECO fuel for UO_2 fuel can result in a *reduced* uranium cost. The cost of a reload will reflect manufacturing costs as well. Manufacturing costs are typically reported in dollars per

kilogram of uranium. Table 4 provides the total mass of uranium per fuel batch, so it can be seen that the reduction in uranium cost for UO_2–BeO fuel is sufficient to offset an increase in manufacturing cost of nearly \$20/kg U.

The economic impact of using ECO fuel extends beyond the fuel cost. The improved thermal performance of the fuel could support less restrictive peaking, operating, and maneuvering limits, and less restrictive limits can contribute to the economic performance of a power plant.

8. Industrial hygiene for BeO and UO_2

A potential disadvantage of ECO fuel is that airborne particulate BeO can cause chronic beryllium disease. This section reviews regulatory limits on exposure to beryllium and uranium, discusses the relative amounts of airborne BeO and UO_2 that would be produced from pellet grinding, and draws qualitative conclusions about the difficulty of complying with regulations for occupational exposures to these materials. It is concluded that, with regard to industrial hygiene, grinding UO_2–BeO fuel pellets may be practicable.

Fuel manufacturers must comply with regulatory limits on occupational exposures when UO_2 fuel pellets are ground to size, but it is not immediately clear whether grinding a UO_2–BeO pellet would require a significant improvement in dust control. A quantitative evaluation of regulatory limits is needed.

Title 10 Code of Federal Regulations Part 850 (10 CFR 850) requires that employers set an action level that is no greater than 0.2 $\mu g/m^3$ for exposure to beryllium, calculated as an 8-h time-weighted average exposure (10 CFR 850.23(a)). Higher levels of exposure are allowed in principle, but they require a significantly increased beryllium monitoring program. Employers may therefore prefer to restrict exposures to below the action level in order to simplify their safety programs.

Exposure to uranium is controlled by both chemical and radiological regulations. Only the radiological regulations (10 CFR 20) will be considered here because they are the more stringent of the two. In 10 CFR 20, the allowable concentration is expressed in terms of the derived air concentration or DAC. One DAC is the concentration in air that, if breathed for a working year of 2000 h, results in a committed effective dose equivalent of 5 rems (0.05 Sv) (whole body) or a committed dose equivalent of 50 rems (0.5 Sv) to any individual organ or tissue. For UO_2 that contains the three uranium isotopes typically present in fresh fuel (^{234}U, ^{235}U, and ^{238}U), one DAC is 2×10^{-11} $Ci/m^3 = 0.74$ Bq/m^3 (10 CFR 20, App. B).

Converting DACs to mass concentrations requires the specific activity of uranium. Enrichment processes change the concentrations of both ^{234}U and ^{235}U in a predictable way, so 10 CFR 20, App. B provides the following formula for the specific activity of enriched uranium:

$$S = (0.4 + 0.38E + 0.0034E^2) \times 10^{-6} \text{ Ci/g}, \quad (1)$$

where S is the specific activity and E is the enrichment expressed in wt% ^{235}U. Commercial fuel facilities are typically licensed for up to 5% ^{235}U, and specific activity increases with enrichment, so it is conservative to evaluate the specific activity for an enrichment of 5%. The resulting specific activity is 2.39×10^{-6} Ci/g. One DAC for 5% enriched UO_2 is therefore 8.4 $\mu g\ U/m^3$.

The relative concentrations of airborne beryllium and uranium will depend on the mass fractions of Be and U in the pellet and on the respirable fraction of grinding dust for each element. The respirable fractions for the UO_2 and BeO phases for pellet grinding are not known, so it will be assumed that they are equal. Under this assumption the concentrations of airborne beryllium and uranium are proportional to the mass fractions of Be and U, respectively, in the fuel pellet. If the volume fraction of BeO in a UO_2–BeO fuel pellet is 10%, the ratio of the mass fractions of Be and U is 0.0125. One DAC of airborne uranium is therefore expected to correspond to 0.105 $\mu g\ Be/m^3$ or about half of the action level for beryllium. Uranium levels in a fuel plant are expected to be well below one DAC, so it appears that grinding UO_2–BeO fuel pellets may be practicable.

9. Summary and conclusions

The behavior of ECO fuels has been investigated with fuel performance and neutronics codes and compared to the behavior of standard UO_2 fuel. The ECO fuel was required to provide the same lifetime energy extraction per fuel assembly and the same core thermal power as standard fuel. For calculations of fuel performance, increasing the linear power of the fuel rod but transferring the extra power directly to the coolant provides a realistic simulation of the presence of a non-fissile, high-conductivity phase such as BeO. Increasing the thermal conductivity by as little as 5% or 10% provide significant benefits in terms of lowered volume-averaged fuel temperature, fission gas release, and fuel rod internal pressure.

BeO was the only workable high conductivity phase investigated for UO_2. Its effects on the neutronics of a fuel assembly were also studied. The criterion used for comparing ECO fuel and standard UO_2 fuel was that the two should have the same k_{inf} and energy extraction per fuel assembly at end of life. The presence of BeO in the ECO fuel necessarily displaces some uranium and therefore decreases the uranium loading of a fuel assembly. Although it might be expected that a significant increase in ^{235}U enrichment would be required to offset the loss of uranium, neutronic calculations showed that the required increase in enrichment is only about 0.007%. Because of the smallness of this change, significant reductions in uranium cost may be possible.

The work reported here provides valuable insights concerning the effect of adding BeO to nuclear fuel. Additional insight could be gained by calculations that reflect more detailed design considerations, such as zone loading with standard and ECO fuels.

Acknowledgement

The authors gratefully acknowledge the support of the US Department of Energy under NERI Project 02-180.

References

[1] J. Fourcade et al., J. Nucl. Mater., these Proceedings.
[2] S. Ishimoto et al., J. Nucl. Sci. Technol. 33 (1996) 134.
[3] Framatome ANP, BAW-10231(NP)-A, Rev. 1, January 2004. <http://adamswebsearch.nrc.gov/scripts/securelogin.pl> under accession numbers ML042930240 and ML042930247.
[4] American Nuclear Society, ANSI/ANS-57.5-1996, 1996.
[5] M. Edenius, A. Ahlin, Studsvik, NFA-86/7, 1986.
[6] Oak Ridge National Laboratory, NUREG/CR-0200, Rev. 6 (ORNL/NUREG/CSD-2/R6), vols. I, II, III, May 2000.
[7] United States Enrichment, SWUcalc, SWU Calculator for Windows, ver. 2.00, 1995.